

Do-Undo: Generating and Reversing Physical Actions in Vision-Language Models

Shweta Mahajan^{*} Shreya Kadambi^{*} Hoang Le Munawar Hayat Fatih Porikli
Qualcomm AI Research[†]

Abstract

We introduce the *Do-Undo* task and benchmark to address a critical gap in vision-language models: understanding and generating physically plausible scene transformations driven by real-world actions. Unlike prior work focused on object-level edits, *Do-Undo* requires models to simulate the outcome of a physical action and then accurately reverse it, reflecting true cause-and-effect in the visual world. We curate a large-scale dataset of reversible actions from real-world videos and design a training strategy enforcing consistency for robust action grounding. Our experiments reveal that current models struggle with physical reversibility, underscoring the importance of this task for embodied AI, robotics, and physics-aware generative modeling. *Do-Undo* establishes an intuitive testbed for evaluating and advancing physical reasoning in multimodal systems.

1. Introduction

Recent advances in vision-language models (VLMs) have enabled remarkable progress in text-driven image synthesis and editing [5, 10, 13, 14, 23, 28], with new capabilities in creative applications and synthetic data generation. Despite these advances, current models remain fundamentally limited in their ability to understand and simulate the physical dynamics of real-world scenes [1, 2, 15, 19, 22]. Most existing approaches focus on object-level manipulations, such as adding or removing objects, while neglecting the underlying cause-and-effect relationships that govern physical interactions [4, 35, 36].

For VLMs to be effective synthetic data generators in real-world applications such as in robotics and in embodied AI agents [3, 21, 27, 34], it is essential that they comprehend how physical actions transform the environment and generate images that plausibly reflect these changes. To make VLMs *physics aware* on classical mechanical manip-

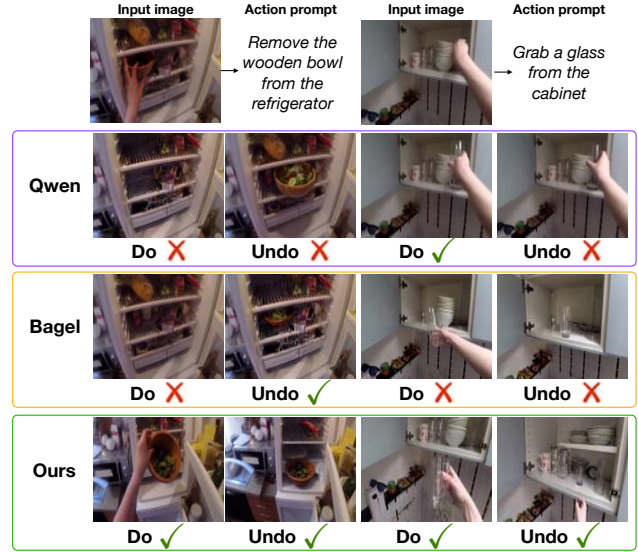


Figure 1. Action-conditioned image generation on the *Do-Undo* dataset highlights a key limitation of current vision-language models: their inability to reverse previously executed actions. Models trained with *Do-Undo* dataset show improved understanding of physical actions and their effects on scene dynamics.

ulations, they should be able to generate the final state without observing a continuous sequence as in video models [29, 31]. For example, given an image with an open refrigerator in a kitchen setting in Figure 1 and the action prompt “remove the wooden bowl from the refrigerator”, the model should be able to simulate a scene with a removed bowl without having to observe the entire sequence of removing the bowl. Furthermore, the image should preserve the dynamics and physical properties of the original scene. For image generation models, this implies modeling the cause-effect relationships by observing the current image and the action in the form of a text or instruction prompt, and generating the final state image.

Recent work on instruction-based image editing [14, 28] has primarily focused on the addition or removal of individual objects; or on maintaining physical properties such as lighting and reflections [6, 24]. However, these approaches

^{*}Equal contribution.

[†]Qualcomm AI Research is an initiative of Qualcomm Technologies, Inc.

often overlook the manipulation of actions, where specific objects undergo transformation or state changes as a result of an action, while the rest of the scene remains unchanged—a property that is essential for synthesizing images reflecting realistic action-driven modifications. On the other hand, action-conditioned image editing models that generate the final state directly from the input image and instruction prompt, do not take into account adherence to physical state of the scene image and require minimal camera movement to preserve background coherence [29].

In this work, we identify a fundamental limitation in current image generation models: the inability to generate action-consistent images and to understand the relationship between actions and object states. For instance, as illustrated in Fig. 1, for the input image and the action prompts “remove the wooden bowl from the refrigerator” or “grab a glass from the cabinet, even state-of-the-art large multimodal models like Qwen-Image [25] and BAGEL [10], struggle to generate physically consistent images, where the models either generate or hallucinate new objects, or are unable to reverse the action that they performed.

To address this gap, we propose the Do-Undo task and benchmark, which challenges models to generate images that accurately reflect the outcome of a physical action, and then to reverse the action. We curate a large-scale dataset of reversible actions from real-world videos and develop a training strategy that enforces consistency, encouraging robust action grounding and physical reasoning. We hypothesize that a good action-aware image generation model should be able to reverse an action that it has just performed and generate physically-consistent images. Through comprehensive evaluation, we demonstrate that current state-of-the-art models struggle with this task, highlighting the need for new approaches to advance physics-aware generative modeling. Moreover, our reversible formulation accommodates dynamic scenes and camera movements, allowing models to generate diverse and plausible final images, provided they can return to the original state by undoing the current action. By establishing the Do-Undo benchmark, we aim to set a new testbed for developing and evaluating VLMs capable of understanding and generating the physical world, thus advancing research in reliable embodied agents.

To summarize, our contributions are: (i) We propose a novel task, *Do-Undo*, by defining reversible physical actions that require the models to generate an image resulting from a physical action and then reverse that action to return to the original scene. (ii) We curate a large-scale dataset of reversible actions from real-world videos in EpicKitchens dataset [9] and design specialized prompting strategy to ensure physically consistent visual generation. Our benchmark accommodates dynamic scenes and camera movements and encourages models to generate diverse yet reversible images. (iii) We develop a baseline

based on BAGEL [10], trained on our proposed benchmark with a consistency loss that ensures reverse actions aligned with the input images. (iv) We demonstrate that current state-of-the-art models struggle with the Do-Undo task by evaluating their performance on the Do-Undo benchmark across different metrics, highlighting the need for physics-aware generative modeling approaches.

2. Related Work

VLM-based image generation and editing. Unified vision-language models [8, 10, 13, 17, 33] for joint understanding and generation of images and text demonstrate impressive results in text-based image editing. BAGEL [10] with its interleaved training strategy for understanding and generation can be applied to image editing tasks. FluxKontext [17] introduces a unified image generation and editing framework based on rectified flow matching. Qwen-Image [33] extends the Qwen-VL [32] understanding model to image generation in a multi-task training with Qwen-VL [32] for image understanding and a variational encoder (VAE) for image generation. This enforces semantic coherence and high fidelity in image editing. Generation chain of thought (GoT) [11] proposes a reasoning-guided paradigm for image generation and editing, incorporating both vision-text understanding and a semantic spatial module. In addition to open models, proprietary models including Gemini [13] and GPT-5 also provide image editing functionality. In this work, we evaluate the advanced VLMs for physics awareness with our Do-Undo benchmark.

Text-based image editing datasets. Text-based image editing datasets such as InstructPix2Pix [5], EMU-Edit [28] and HQ-Edit [14] introduced synthetic datasets for instruction-based image editing. InstructPix2Pix and EMU-Edit provide open-domain instructions on synthetic and real images respectively. SEED-DataEdit [12] extends text-guided image editing to multi-turn scenarios. MagicBrush [36] provides an instruction-guided real image supporting single-turn, multi-turn, mask-provided, and mask-free editing. However, these datasets lack action-guided editing instructions that reflect changes based on physical actions performed on objects.

To evaluate instruction-based editing, Magicbrush provides a test set with and without masks as additional guidance for single and multi-turn editing. EMU-Edit extends MagicBrush with more challenging instructions, covering categories such as background and style manipulation, object removal and addition, texture changes, and global image modifications. These benchmarks employ metrics such as CLIP [26], ℓ_1 , DINO [7] similarity, and human scores.

Action-aware image editing. GenHowTo [29] and Aurora [16] are the two action-centric editing datasets. GenHowTo samples frames from action-centric instructional

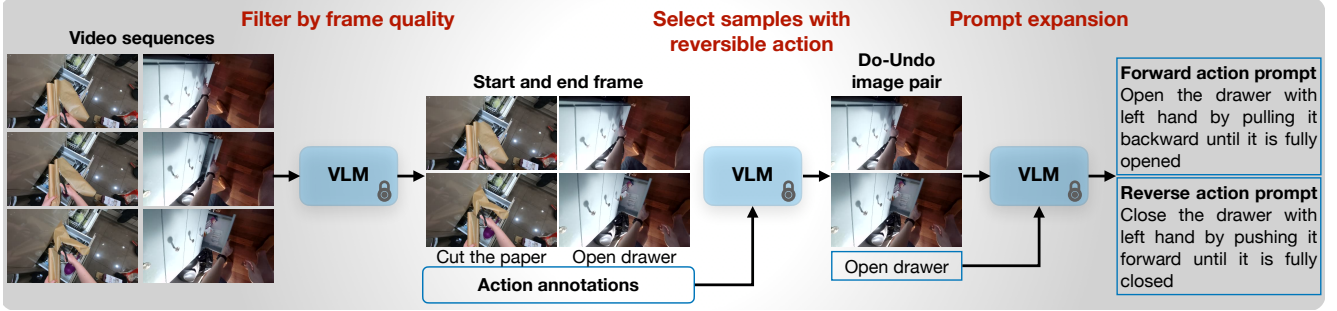


Figure 2. **Do-Undo data curation pipeline.** Starting with the EpicKitchens dataset [9], we select visually high quality samples which have reversible actions; the action annotations and the images are used to expand the prompts with additional visual context.

videos with their captions starting from input image (which may or may not contain the target objects on which action is being performed) to an image showing action being performed and the final state. The dataset introduces new objects in the scene causing considerable drift from the input image limiting application to action-based image editing. Aurora [16] covers a wide range of actions where the input and final state images share the same visual context, but often lack explicit causal clues, such as the presence of a person or hand manipulating objects. Our Do-Undo dataset addresses these limitations by providing high-quality, reversible action pairs with detailed context.

Aurora-bench further includes action-conditioned and reasoning based editing instructions. The benchmark, in addition to the standard editing metrics includes a score where the similarity between the input image and the two images generated with instructions that cause no change and considerable modification are compared to measure the understanding of the instructional prompt by the editing model. Trusca et al. [31] leverages a diffusion model and provides natural language instructions specifying the action from the start frame to the end frame. PICABench [24], introduces a physics-aware benchmark with physical effects such as optics, mechanics, and transitions, for example, in an image with "a person riding a scooter" if the instruction is "remove scooter" then the model should generate a physically plausible image with the person standing and not floating in the air. In our benchmark, we study the action following capabilities of VLM-based editing models on the ability to reverse the action that the model has just performed.

3. Do-Undo Reversible Action-aware Learning

Given an image representing an initial state, our goal is to enable VLMs with capabilities to generate or edit images based on physical actions performed on the objects present in the image *by an agent* or humans. This implies that the underlying VLM should understand the visual content of the input image including the state of the objects and the context; the action to be performed; the physics of action,

object, and agent interaction; and generate physically plausible images after the action is performed.

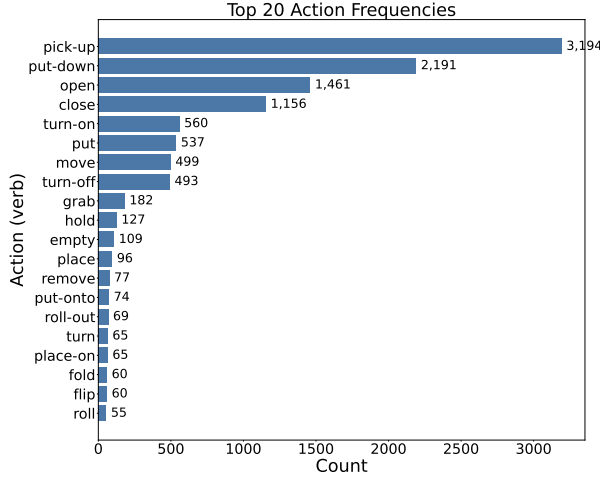
To encode actions in VLMs, we design action prompts with a special prompting strategy which provides the VLM with the current visual context and the action description. Importantly, to endow the models with the capability of understanding the physics of the world under actions, we design the novel task and benchmark called *Do-Undo*. We define a set of actions for physical manipulation of objects such that the actions have their reversible counterparts. A *forward action* takes the image from the input state to the state after the action is performed. The actions are reversible if the image in the final state based on the action prompt can be brought back to the original state in a physically plausible manner. For example, the action "open the door" can be reversed with "close the door", however, the action "open a bag of chips" may not be reversed. By introducing reversible actions, we ensure that the models can come back to their original state, thereby inducing action conditioned image understanding priors in the VLMs.

In the following section, we describe the dataset curation procedure to train VLMs in our Do-Undo setup for physics-aware action-conditioned image generation.

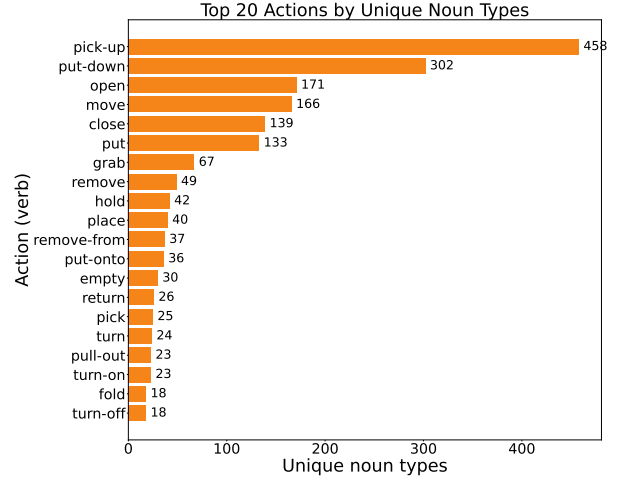
3.1. The Do-Undo Dataset

With the goal to achieve physics-aware image generation with action prompts, we need to mine datasets that have natural image and action scenarios, for example, manipulating and performing a task in kitchen environment. The data set should include an interaction between a human or agent and the objects on which the action is applied, and the action performed is reversible with a naturally plausible return to the original state. We collect a set of tuples (I_o, P_F, I_F, P_R) with I_o being the input image, I_F is the image after the action has executed, P_F is the forward action prompt, and P_R is the reverse action prompt.

Image-pair acquisition. To collect the image pairs I_o and I_F , which in addition to the input image and the final state image, also have real image scenes with humans per-

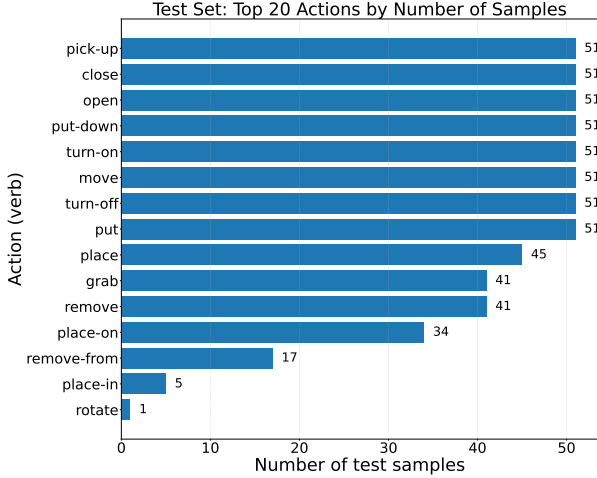


(a) Number of samples for top-20 reversible actions in the training set.

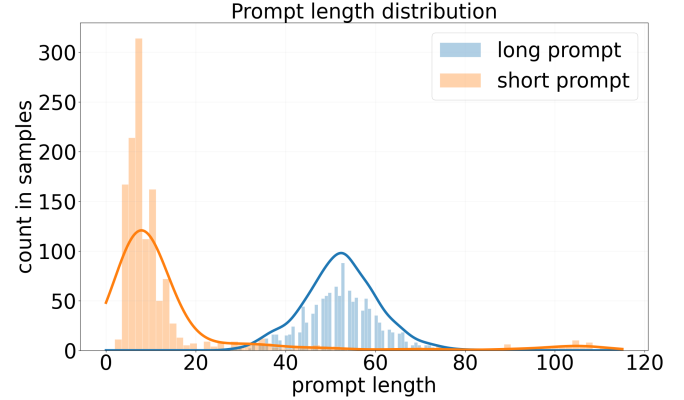


(b) Number of unique nouns or objects for each action in the training set.

Figure 3. **Dataset statistics of our Do-Undo training set.** We generate data by mining reversible tasks from EpicKitchens [9] dataset. (left) We show the distribution of top-20 actions in the training data. (right) We analyze the diversity in the unique objects handled when performing each action.



(a) Number of samples and actions in the test set.



(b) Prompt expansion and short prompt statistics on the test set.

Figure 4. **Dataset statistics of our Do-Undo test set.** (left) We show the distribution of actions in the test data. (right) The test set includes long and short prompts to account for the sensitivity of different VLMs to prompt length.

forming actions in a real-world setup, we rely on the Epic Kitchens video dataset [9]. EpicKitchens consists of 100 video episodes with subsequences comprising video frames from start to end of action. The videos feature humans performing everyday tasks in kitchen environment recorded with an ego-centric camera set-up providing real-world, first person perspective. We sample the start and end frames from the video sequences demonstrating start of the action and end of the action, respectively. To curate high quality samples for physics-aware image editing and generation, we use the action annotations provided in the EpicKitchens dataset and employ Qwen-VL [32] to check for consistency

between the start and end frames. For this, given the start, end and action annotation such as “open the door”, we instruct the model to score 0 or 1: if the frames are visually clear with respect to the light conditions and blur, if the object is present in both the start and end frame, if the action annotation is correctly applied from start to end frame *i.e.* (partially) closed door to open door state in the example.

Reversible actions. We first list a set of action vocabulary with their physically plausible reverse actions including *pick-up*, *put-down*, *put*, *open*, *grab*, *turn-off*, *turn-on*, *close*, *put-down*, *place*, *move*, and *remove*. It is worth noting that the action and its reverse can be in any order. That

is, a “turn-on” action can happen before “turn-off” action or vice-versa. Moreover, different action descriptions can have a same inverse. In our case, “grab” and “pick-up” forward actions can be reversed with “put” or “put-down” reverse action. From the clean image-pairs, we consolidate the samples with these action annotations.

Forward and reverse action prompt expansion. Since Epickitchens [9] contains action annotations only, to make the dataset compatible for action-based instruction following in vision-language models, we design a prompt expansion strategy with the goal to provide the model with additional visual context of the input image and the action description. To construct the forward action prompt P_F , we provide Qwen-VL [32] model with five temporally sampled frames of the sequence and the action annotation and instruct the model to generate a prompt that follows the $\langle \text{verb}, \text{object} \rangle$ format of the original action annotation, is more descriptive, includes the details of the object being interacted with, includes the detail of person’s hand (one hand, two hands, posture, left or right hand), includes the spatial relationship between the object and the human. Analogously, we provide the frames in reverse order and provide the same instructions to create the reverse prompt P_R to undo the action. These action prompts guide the VLM for precise image editing while accounting for the variations in camera movements or the background mismatch between the start and the end images. The complete instruction prompt is provided in the appendix.

Dataset statistics. After filtering the EpicKitchens dataset with reversible actions, we obtain 24,000 samples in the training set including both the forward and reverse action pairs. In Figure 3, we analyze the samples from the training data. We observe that certain actions are more pronounced with pick-up forming almost 26% of the training data (Figure 3a). However, the joint vocabulary of action (verb) and object (nouns) $\langle \text{verb}, \text{object} \rangle$ pairs provide sufficient sample diversity (cf. Figure 10).

For the test set, we ensure balance across the actions with a total of 662 samples. As shown in Figure 4a, the top-8 classes are represented equally. We also include *out-of-distribution* classes—rotate, remove-from and stack, to test the physics-awareness of any physical manipulation task. Noting that vision-language models are sensitive to the prompt length with models like Qwen-Image and BAGEL performing well on short and long descriptions respectively; we provide long and short descriptions of the forward and the reverse actions to benchmark physics-aware generative editing to cater for different models (Figure 4b).

3.2. Training on Do-Undo

We assume a vision-language model (VLM) with the capability to generate both images and text in an interleaved setup; \mathcal{E}_θ parameterized by θ that takes as input an image

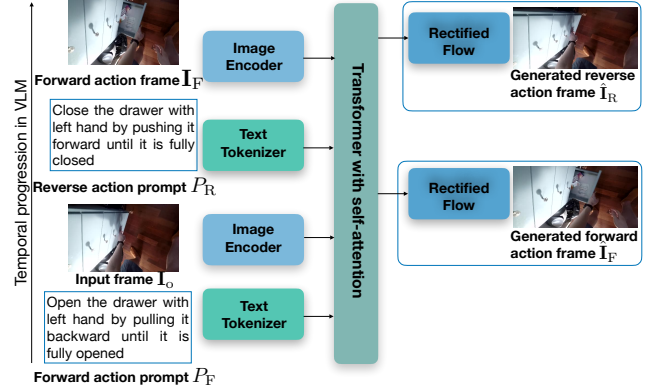


Figure 5. **Do-Undo with BAGEL.** Architecture of our approach with BAGEL [10] as the VLM.

and prompt to generate images. By training a VLM on our *Do-Undo* dataset our goal is to induce physics aware generation grounded in actions by enforcing consistency between the forward and the reverse actions.

In our work, we consider BAGEL [10] as the underlying VLM. It is based on the large language model decoder-only transformer (Qwen 2.5) [25] and includes the efficient KV caching mechanism for image generation. The model has two visual encoders: a ViT for encoding visual features for image understanding and a pretrained VAE encoder [18] for encoding images from pixel to latent space with spatial dimension downsampled by factor of 8 resulting in 16 channels. To make these latents compatible in the LLM backbone, they are further patchified to match the hidden dimension of LLM.

Our training data consists of tuples (I_0, P_F, I_F, P_R) . Let $I_0 \in \mathbb{R}^{H \times W \times 3}$ be an input image and P_F be a reversible action prompt describing a physically meaningful manipulation of objects in I_0 (e.g., “open the drawer with left hand by pulling it backward until it is fully opened”) as shown in Fig. 5. We first encode P_F and I_0 using a text tokenizer and a ViT respectively. The combined features form the context for the subsequent generation of frame I_F . Rectified flow matching is employed as a conditional image generation model minimizing the mean squared error (MSE) for noisy encoding of I_F with a VAE encoder yielding \hat{I}_F .

During training for the reverse direction, we encode the reverse action prompt P_R and the groundtruth image I_F into the VLM which serve as the conditioning or context for generating the reverse image \hat{I}_R . Notably, the generated undo image should be the same as the input image I_0 . Therefore, for generating the reverse image with rectified flow, we minimize the MSE with the noisy latent from I_0 to get \hat{I}_R . We follow the finetuning strategy of the original model [10] for multimodal understanding and generation tasks, of text-to-image generation on the image-text-pair set; *interleaved training on our Do-Undo dataset* and multimodal under-

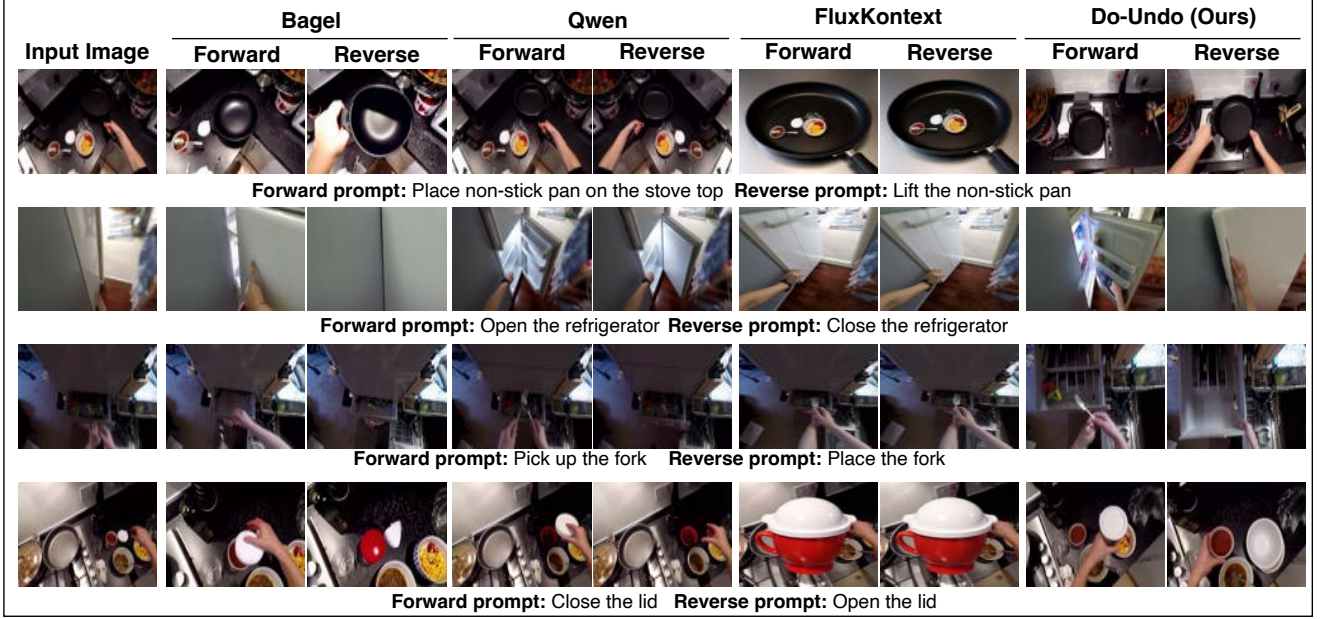


Figure 6. **Qualitative results for different actions.** Qualitative results across “pick-up”, “place”, “open” verbs on Qwen Image [33], FluxKontext [17], Bagel [10] and Do-Undo (Ours).

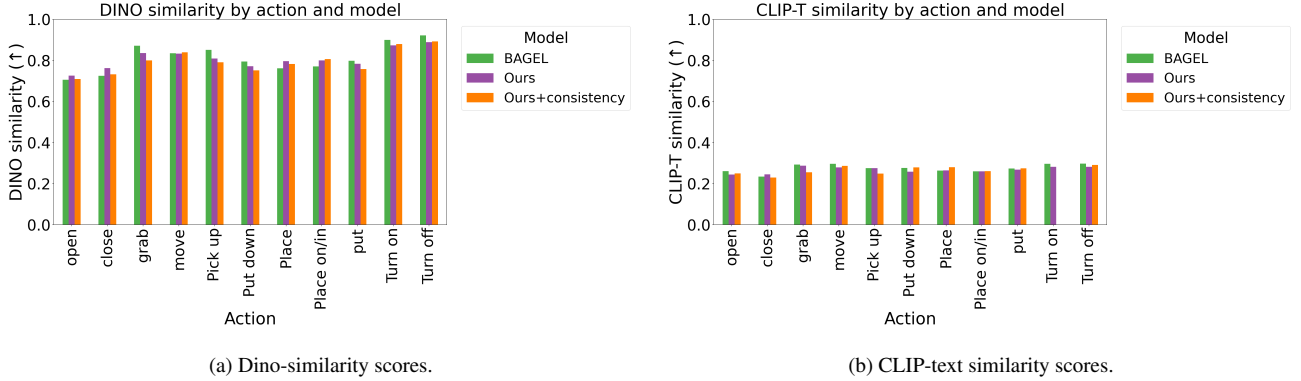


Figure 7. **Quantitative results on Do-Undo benchmark.** We evaluate baseline BAGEL with the model trained on Do-Undo training data (Ours) and with the consistency loss (Ours+consistency). Incorporating Do-Undo training improves action-following while preserving image faithfulness on both action and start frame across tasks such as *close*, *open*, *move*, *place*, and *place-in*.

standing on the instruction finetuning set from BAGEL [10]. The model is trained on the mean-squared error from rectified flow matching and the cross-entropy loss for next-token prediction to generate text.

Do-undo consistency. To make the VLM \mathcal{E}_θ physics-aware when generating action-conditioned images, in addition to training on our dataset, we enforce a consistency loss on the input image \mathbf{I}_0 and $\hat{\mathbf{I}}_R$ such that $\hat{\mathbf{I}}_R \approx \mathbf{I}_0$. We hypothesize that if a VLM truly understands action conditions, it should be able to generate a close approximation of the original image and therefore, during training, we enforce:

$$\mathcal{L}_c = \|\mathbf{I}_0 - \hat{\mathbf{I}}_R\|_1. \quad (1)$$

4. Experiments

To investigate the performance of large-scale vision-language models for physics-aware generation, we evaluate BAGEL [10], Qwen-Image-2509 [33] and Flux-Kontext [17] on our proposed *Do-Undo* benchmark. Additionally, we assess qualitative performance on Gemini [13].

Evaluation metrics. We validate the performance on a diverse set of metrics, each catering to a different aspect of the physics-aware action-conditioned image generation. We include (i) DINO-R that measures the image similarity between the reverse image $\hat{\mathbf{I}}_R$ and the original input image \mathbf{I}_0 . It evaluates the ability of a model to return to its original

Table 1. **Quantitative evaluation with prompt expansion.** Evaluation of different VLMs on our Do-Undo test dataset with prompt expansion. Lower DINO-F scores indicate that models make partial edits rather than completing actions. This tendency to preserve the initial frame is also reflected in lower CLIP scores.

Method	DINO-R \uparrow	DINO-F \uparrow	CLIP-T-R \uparrow	CLIP-T-F \uparrow	EPE (OF) \downarrow	OF-F \downarrow
Qwen-Image [25]	0.861	0.788	0.196	0.188	0.050	78.78
Bagel [10]	0.812	0.770	0.274	0.275	0.102	79.20
Flux Kontext [17]	0.797	0.757	0.253	0.277	0.120	79.20
Do-Undo	0.807	0.764	0.268	0.270	0.122	85.40
Do-Undo(c)	0.795	0.744	0.264	0.265	0.113	84.05

Table 2. **Quantitative evaluation with short prompts.** Evaluation of different VLMs on our Do-Undo FULL test dataset with short prompts. We observe that Qwen and FluxKontext are more sensitive to the prompt length compared to Bagel and our model.

Method	DINO-R \uparrow	DINO-F \uparrow	CLIP-T-R \uparrow	CLIP-T-F \uparrow	EPE (OF) \downarrow	OF-F \downarrow
Qwen Image [25]	0.882	0.783	0.284	0.287	0.061	82.57
BAGEL [10]	0.806	0.758	0.270	0.277	0.102	72.08
Flux Kontext [17]	0.795	0.727	0.263	0.266	0.122	83.68
Do-Undo	0.810	0.768	0.268	0.269	0.121	84.00
Do-Undo(c)	0.800	0.748	0.262	0.263	0.116	82.00



Figure 8. **Generalization to object-action interaction for Do-Undo task on rare annotations.** Our Do-Undo model preserves hand-object interaction and correctly emulates grasping actions, even for rare annotations.

state. (ii) Similarly, DINO-F measures the similarity between the generated forward image $\hat{\mathbf{I}}_F$ and the ground-truth \mathbf{I}_F . (iii) We measure the semantics of the generated forward and reverse images by measuring the similarity between the generated images and the captions generated from the respective ground-truth images with CLIP-T-R and CLIP-T-F scores. CLIP-T-R measures the similarity between the generated reverse image and the caption generated for the original image. Analogously, CLIP-T-F measures similarity between the generated forward image and the caption from the corresponding ground-truth forward image. (iv) We include end point error (EPE (OF)) using RAFT [30] for optical flow. For this, we compute the forward optical flow as the error between the input image and the forward, and the reverse optical flow as the error between the reverse image and the forward image. We then compute the difference between the forward optical flow error and the backward optical flow error. In an ideal case when the reverse image is same as the original image, the EPE will be zero. We also report optical flow error (OF-F) as the optical flow error between the ground truth forward image and the generated forward image. (v) Finally, we employ Gemini (VLM) as a judge to assess the instruction-following and semantic consistency of generated images. Specifically, we prompt a vi-

sion-language model to evaluate whether the generated images accurately reflect the intended actions described in the prompts. The VLM provides scores for instruction fidelity (IF), object identity preservation (IDP), temporal coherence (TC), and object consistency (OC). (vi) We also include a human preference evaluation in Table 7 in the appendix.

Quantitative results. In Tables 1 and 2, we perform the zero-shot evaluation of the different VLMs on *Do-Undo* benchmark with our prompt expansion (long prompts) and short prompts. Additionally, we report results for BAGEL trained on our dataset(Do-Undo), as well as with an added consistency loss (DO-Undo (c)) to further align the reverse action image with the original input. We observe BAGEL has a better trade-off between faithfulness and action-image alignment for image-based metrics *i.e.* DINO-R, DINO-F and EPE(OF), compared to other state-of-the-art models like Qwen-Image and Flux Kontext when provided with long prompts. This can be attributed to the special training procedure of the underlying model, with the ability to understand the texts during interleaved editing. For shorter prompts in Table 2, Qwen-Image has better performance than BAGEL, highlighting sensitivity to prompt length for different VLMs. When trained on our data, BAGEL with Do-Undo has high CLIP-T-R similarity, showing that the

Table 3. **MLLM (Gemini 2) as judge.** Our D-Undo approach improves Instruction following while preserving the identity.

Method	Instruction (IF) \uparrow	Identity (IDP) \uparrow	Temporal (TC) \uparrow	Object consistency (OC) \uparrow
Qwen Image [25]	8.44	9.35	8.15	9.18
Bagel [10]	7.97	9.30	8.17	9.26
FluxKontext [17]	6.69	8.82	6.91	8.81
Do-Undo	8.05	9.12	8.03	9.06
Do-Undo(c)	8.02	9.11	7.94	9.09

Table 4. **MLLM (Gemini 2.5) as judge on different actions.** Do-Undo improves over BAGEL on the Instruction following (IF) while keeping identity this providing good trade-off on long prompts not only on well represented classes but also on rare classes like Place-on.

Method	Metric	pick-up	put-down	open	close	turn-on	move	turn-off	grab	place	place-on
Bagel [10]	IF	8.190	8.600	8.390	8.960	7.999	7.660	6.450	7.430	8.130	7.920
	IDP	8.860	9.900	9.720	9.190	9.150	8.960	9.520	8.490	9.450	9.800
Do-Undo	IF	8.520	8.820	8.720	8.110	7.860	8.660	6.030	8.370	6.940	8.510
	IDP	8.705	9.590	9.130	9.370	9.000	9.430	8.960	8.230	9.090	9.700

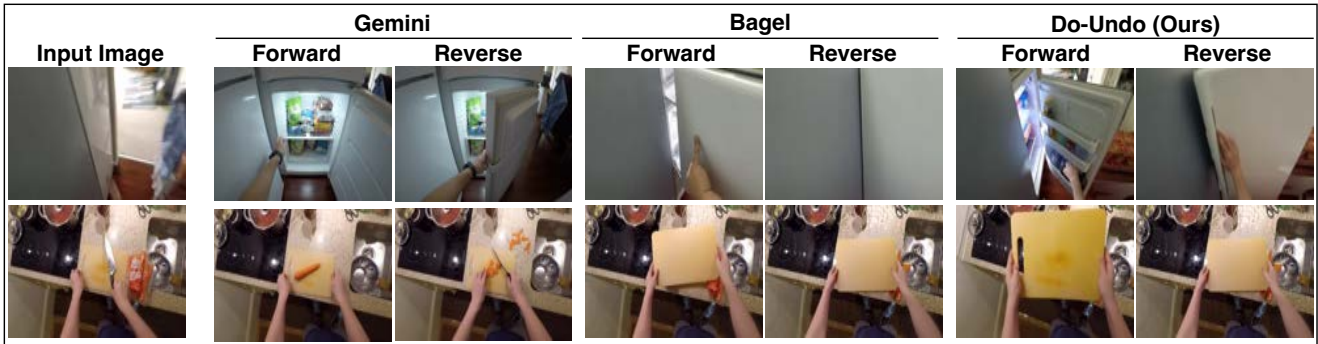


Figure 9. **Hallucination of objects during action conditioned generation.** (top): A person’s left hand opens the lower white freezer door of a refrigerator, revealing its interior. (bottom): Pick up yellow rectangular chopping board with both hands from a speckled countertop.

model with our data generates content with high semantic similarity in the reverse image. On analyzing the DINO-R scores closely in Figs. 7a and 7b, we find that while our Do-Undo model has a lower average score, we outperform BAGEL on per-action classes scores except on “pick-up” and “grab”. This can be due to class imbalance in our training set with the potential of the model (depending on its training strategy) to overfit on certain classes. To account for variations in camera motion, unusual hand grasp etc., we report Gemini as a judge scores Tab. 3, Tab. 4 on zero-shot performance. While both BAGEL and Qwen preserve the identity of target and non-target objects, BAGEL performs worse on instruction following. Models like Flux break the temporal consistency and contextual coherence.

Qualitative results. In Fig. 6 we show the qualitative results from BAGEL, Qwen-Image, FluxKontext and our Do-Undo model for different real kitchen scenes. The state of the art models fail to be faithful to the content of the input image, at times generating new objects which are not present in the original image. The models also are unable to perform the reverse task. Notably our approach can perform the forward and the reverse tasks across samples and also adheres to the hand movement in object-human inter-

action (e.g. row 2, Fig. 6). In Fig. 8, we show the ability of our model to generate action-conditioned images for the actions that are rare in the training set. This shows that our model can induce physical understanding as an emergent property in vision-language models. Additionally, in Fig. 9, we consistently observe that models like Gemini tend to hallucinate and create new objects. Our approach and dataset addresses these limitations and our model is consistent with the visual context of the input image.

5. Conclusion

In this paper, we introduced Do-Undo, a new task and benchmark to address the limitations of vision-language models in their ability to understand and generate physically plausible images based on real-world actions. Do-Undo emphasizes the cause-effect reasoning for generating synthetic data by requiring the model to generate the forward action and then reversing it to go back to original state. Through our extensive experiments, we demonstrated that even the best performing models struggle with physically plausible reversible actions and often hallucinate new objects or fail to maintain scene consistency. We believe that our new task and benchmark serve as an important testbed for the development of physics-aware generative models.

References

- [1] Haider Al-Tahan, Quentin Garrido, Randall Balestriero, Diane Bouchacourt, Caner Hazirbas, and Mark Ibrahim. Unibench: Visual reasoning requires rethinking vision-language beyond scaling. *Advances in Neural Information Processing Systems*, 37:82411–82437, 2024. 1
- [2] Alisson Azzolini, Junjie Bai, Hannah Brandon, Jiaxin Cao, Prithvijit Chattopadhyay, Huayu Chen, Jinju Chu, Yin Cui, Jenna Diamond, Yifan Ding, et al. Cosmos-reason1: From physical common sense to embodied reasoning. *arXiv preprint arXiv:2503.15558*, 2025. 1
- [3] Apratim Bhattacharyya, Mateusz Malinowski, Bernt Schiele, and Mario Fritz. Long-term image boundary prediction. In *Proceedings of the AAAI Conference on Artificial Intelligence*, 2018. 1
- [4] Anand Bhattad, Konpat Preechakul, and Alexei A Efros. Visual jenga: Discovering object dependencies via counterfactual inpainting. *arXiv preprint arXiv:2503.21770*, 2025. 1
- [5] Tim Brooks, Aleksander Holynski, and Alexei A Efros. Instructpix2pix: Learning to follow image editing instructions. In *Proceedings of the IEEE/CVF Conference on Computer Vision and Pattern Recognition*, pages 18392–18402, 2023. 1, 2
- [6] Ziqi Cai, Shuchen Weng, Yifei Xia, and Boxin Shi. Physedit: Physics-aware semantic image editing with text description. In *2025 IEEE/CVF Conference on Computer Vision and Pattern Recognition*, pages 7867–7876, 2025. 1
- [7] Mathilde Caron, Hugo Touvron, Ishan Misra, Hervé Jégou, Julien Mairal, Piotr Bojanowski, and Armand Joulin. Emerging properties in self-supervised vision transformers. In *Proceedings of the IEEE/CVF International Conference on Computer Cision*, pages 9650–9660, 2021. 2
- [8] Jiu hai Chen, Zhiyang Xu, Xichen Pan, Yushi Hu, Can Qin, Tom Goldstein, Lifu Huang, Tianyi Zhou, Saining Xie, Silvio Savarese, et al. Blip3-o: A family of fully open unified multimodal models-architecture, training and dataset. *arXiv preprint arXiv:2505.09568*, 2025. 2
- [9] Dima Damen, Hazel Doughty, Giovanni Maria Farinella, Sanja Fidler, Antonino Furnari, Evangelos Kazakos, Davide Moltisanti, Jonathan Munro, Toby Perrett, Will Price, et al. The epic-kitchens dataset: Collection, challenges and baselines. *IEEE Transactions on Pattern Analysis and Machine Intelligence*, 43(11):4125–4141, 2020. 2, 3, 4, 5
- [10] Chaorui Deng, Deyao Zhu, Kunchang Li, Chenhui Gou, Feng Li, Zeyu Wang, Shu Zhong, Weihao Yu, Xiaonan Nie, Ziang Song, Guang Shi, and Haoqi Fan. Emerging properties in unified multimodal pretraining. *arXiv preprint arXiv:2505.14683*, 2025. 1, 2, 5, 6, 7, 8, 11, 15, 16
- [11] Rongyao Fang, Chengqi Duan, Kun Wang, Linjiang Huang, Hao Li, Shilin Yan, Hao Tian, Xingyu Zeng, Rui Zhao, Jifeng Dai, et al. Got: Unleashing reasoning capability of multimodal large language model for visual generation and editing. *arXiv preprint arXiv:2503.10639*, 2025. 2
- [12] Yuying Ge, Sijie Zhao, Chen Li, Yixiao Ge, and Ying Shan. Seed-data-edit technical report: A hybrid dataset for instructional image editing. *arXiv preprint arXiv:2405.04007*, 2024. 2
- [13] Google DeepMind. Gemini 2.5 flash: Fast and intelligent multimodal model. <https://ai.google.dev/gemini-api/docs/models>, 2025. Accessed: 2025-10-23. 1, 2, 6
- [14] Mude Hui, Siwei Yang, Bingchen Zhao, Yichun Shi, Heng Wang, Peng Wang, Yuyin Zhou, and Cihang Xie. Hq-edit: A high-quality dataset for instruction-based image editing. *arXiv preprint arXiv:2404.09990*, 2024. 1, 2
- [15] Bingyi Kang, Yang Yue, Rui Lu, Zhijie Lin, Yang Zhao, Kaixin Wang, Gao Huang, and Jiashi Feng. How far is video generation from world model: A physical law perspective. *arXiv preprint arXiv:2411.02385*, 2024. 1
- [16] Benno Krojer, Dheeraj Vattikonda, Luis Lara, Varun Jampani, Eva Portelance, Chris Pal, and Siva Reddy. Learning action and reasoning-centric image editing from videos and simulation. *Advances in Neural Information Processing Systems*, 37:38035–38078, 2024. 2, 3
- [17] Black Forest Labs, Stephen Batifol, Andreas Blattmann, Frederic Boesel, Saksham Consul, Cyril Diagne, Tim Dockhorn, Jack English, Zion English, Patrick Esser, Sumith Kulal, Kyle Lacey, Yam Levi, Cheng Li, Dominik Lorenz, Jonas Müller, Dustin Podell, Robin Rombach, Harry Saini, Axel Sauer, and Luke Smith. Flux.1 kontext: Flow matching for in-context image generation and editing in latent space, 2025. 2, 6, 7, 8
- [18] Black Forest Labs, Stephen Batifol, Andreas Blattmann, Frederic Boesel, Saksham Consul, Cyril Diagne, Tim Dockhorn, Jack English, Zion English, Patrick Esser, et al. Flux.1 kontext: Flow matching for in-context image generation and editing in latent space. *arXiv preprint arXiv:2506.15742*, 2025. 5
- [19] Wenbin Li, Aleš Leonardis, and Mario Fritz. Visual stability prediction for robotic manipulation. In *2017 IEEE International Conference on Robotics and Automation*, pages 2606–2613, 2017. 1
- [20] Haotian Liu, Chunyuan Li, Qingyang Wu, and Yong Jae Lee. Visual instruction tuning. *Advances in Neural Information Processing Systems*, 36:34892–34916, 2023. 11
- [21] Cong Lu, Philip Ball, Yee Whye Teh, and Jack Parker-Holder. Synthetic experience replay. *Advances in Neural Information Processing Systems*, 36:46323–46344, 2023. 1
- [22] Fanqing Meng, Jiaqi Liao, Xinyu Tan, Wenqi Shao, Quanfeng Lu, Kaipeng Zhang, Yu Cheng, Dianqi Li, Yu Qiao, and Ping Luo. Towards world simulator: Crafting physical commonsense-based benchmark for video generation. *arXiv preprint arXiv:2410.05363*, 2024. 1
- [23] OpenAI. Gpt-image-1. <https://platform.openai.com/docs/guides/image-generation?image-generation-model=gpt-image-1>, 2025. 1
- [24] Yuandong Pu, Le Zhuo, Songhao Han, Jinbo Xing, Kaiwen Zhu, Shuo Cao, Bin Fu, Si Liu, Hongsheng Li, Yu Qiao, et al. Picabench: How far are we from physically realistic image editing? *arXiv preprint arXiv:2510.17681*, 2025. 1, 3
- [25] Qwen, :, An Yang, Baosong Yang, Beichen Zhang, Binyuan Hui, Bo Zheng, Bowen Yu, Chengyuan Li, Dayiheng Liu, Fei Huang, Haoran Wei, Huan Lin, Jian Yang, Jianhong Tu, Jianwei Zhang, Jianxin Yang, Jiayi Yang, Jingren Zhou, Junyang Lin, Kai Dang, Keming Lu, Keqin Bao, Kexin Yang, Le

- Yu, Mei Li, Mingfeng Xue, Pei Zhang, Qin Zhu, Rui Men, Runji Lin, Tianhao Li, Tianyi Tang, Tingyu Xia, Xingzhang Ren, Xuancheng Ren, Yang Fan, Yang Su, Yichang Zhang, Yu Wan, Yuqiong Liu, Zeyu Cui, Zhenru Zhang, and Zihan Qiu. Qwen2.5 technical report, 2025. [2](#), [5](#), [7](#), [8](#)
- [26] Alec Radford, Jong Wook Kim, Chris Hallacy, Aditya Ramesh, Gabriel Goh, Sandhini Agarwal, Girish Sastry, Amanda Askell, Pamela Mishkin, Jack Clark, et al. Learning transferable visual models from natural language supervision. In *International Conference on Machine Learning*, pages 8748–8763, 2021. [2](#)
- [27] Hongrui Sang, Rong Jiang, Zhipeng Wang, Yanmin Zhou, Ping Lu, and Bin He. Scene augmentation methods for interactive embodied ai tasks. *IEEE Transactions on Instrumentation and Measurement*, 72:1–11, 2023. [1](#)
- [28] Shelly Sheynin, Adam Polyak, Uriel Singer, Yuval Kirstain, Amit Zohar, Oron Ashual, Devi Parikh, and Yaniv Taigman. Emu edit: Precise image editing via recognition and generation tasks. In *Proceedings of the IEEE/CVF Conference on Computer Vision and Pattern Recognition*, pages 8871–8879, 2024. [1](#), [2](#)
- [29] Tomáš Souček, Dima Damen, Michael Wray, Ivan Laptev, and Josef Sivic. Genhowto: Learning to generate actions and state transformations from instructional videos. In *Proceedings of the IEEE/CVF Conference on Computer Vision and Pattern Recognition*, pages 6561–6571, 2024. [1](#), [2](#)
- [30] Zachary Teed and Jia Deng. Raft: Recurrent all-pairs field transforms for optical flow. In *European Conference on Computer Vision*, pages 402–419, 2020. [7](#)
- [31] Maria Mihaela Trusca, Mingxiao Li, and Marie-Francine Moens. Action-based image editing guided by human instructions. *arXiv preprint arXiv:2412.04558*, 2024. [1](#), [3](#)
- [32] Peng Wang, Shuai Bai, Sinan Tan, Shijie Wang, Zhihao Fan, Jinze Bai, Keqin Chen, Xuejing Liu, Jialin Wang, Wenbin Ge, Yang Fan, Kai Dang, Mengfei Du, Xuancheng Ren, Rui Men, Dayiheng Liu, Chang Zhou, Jingren Zhou, and Junyang Lin. Qwen2-vl: Enhancing vision-language model’s perception of the world at any resolution, 2024. [2](#), [4](#), [5](#)
- [33] Chenfei Wu, Jiahao Li, Jingren Zhou, Junyang Lin, Kaiyuan Gao, Kun Yan, Sheng ming Yin, Shuai Bai, Xiao Xu, Yilei Chen, Yuxiang Chen, Zecheng Tang, Zekai Zhang, Zhengyi Wang, An Yang, Bowen Yu, Chen Cheng, Dayiheng Liu, Deqing Li, Hang Zhang, Hao Meng, Hu Wei, Jingyuan Ni, Kai Chen, Kuan Cao, Liang Peng, Lin Qu, Minggang Wu, Peng Wang, Shuting Yu, Tingkun Wen, Wensen Feng, Xiaoxiao Xu, Yi Wang, Yichang Zhang, Yongqiang Zhu, Yujia Wu, Yuxuan Cai, and Zenan Liu. Qwen-image technical report, 2025. [2](#), [6](#)
- [34] Yandan Yang, Baoxiong Jia, Peiyuan Zhi, and Siyuan Huang. Physcene: Physically interactable 3d scene synthesis for embodied ai. In *Proceedings of the IEEE/CVF Conference on Computer Vision and Pattern Recognition*, pages 16262–16272, 2024. [1](#)
- [35] Yang Ye, Xianyi He, Zongjian Li, Bin Lin, Shenghai Yuan, Zhiyuan Yan, Bohan Hou, and Li Yuan. Imgedit: A unified image editing dataset and benchmark. *arXiv preprint arXiv:2505.20275*, 2025. [1](#)
- [36] Kai Zhang, Lingbo Mo, Wenhui Chen, Huan Sun, and Yu Su. Magicbrush: A manually annotated dataset for instruction-guided image editing. *Advances in Neural Information Processing Systems*, 36:31428–31449, 2023. [1](#), [2](#)

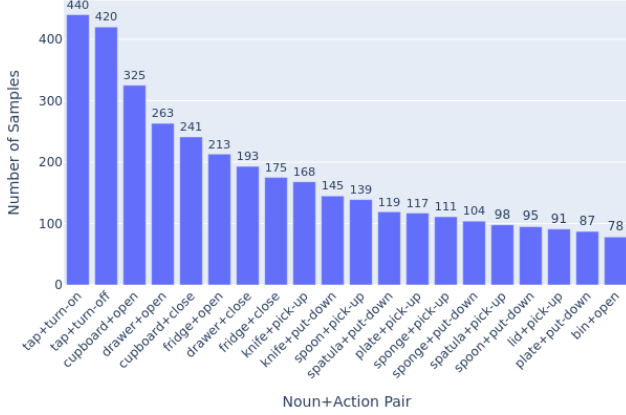


Figure 10. **Training data statistics.** Frequency of joint noun action pairs in the training do-undo dataset. Clearly, even though pick-up as a lone action dominates the actions, the diversity of the action-noun pairs shows a balanced representation of the training data.

A. Training Details

To show the benefits of our Do-Undo training dataset for physics-aware generative image editing, we build upon the unified image understanding and generation model, BAGEL [10], and leverage its interleaved editing training pipeline for finetuning on our Do-Undo data. We start with the pre-trained publically available BAGEL-7B-MoT checkpoint, with 7B parameters and the mixture of transformer experts (MoT) set-up of BAGEL for understanding and generation.

Training Data. The Do-Undo dataset is introduced in the vision-text interleaved data module. The interleaved data is constructed with the input image, a forward action prompt, and the ground-truth final image in order. Similarly, for the reverse undo direction, the sample consists of the ground-truth final image, the reverse action prompt, and the ground-truth input image. Following BAGEL, the following image transformations are applied: image stride: 16, max image size: 1024, min image size: 512. For ViT, we apply: image stride: 14, max image size: 518 and min image size: 224. For text to image generation, we use: image stride: 16, max image size: 1024, and min image size: 512.

During finetuning, in addition to Do-Undo data for interleaved vision-text formulation, we integrate the supervised finetuning as presented in BAGEL with the `llava ov` dataset from LLaVA [20] for vision-language understanding. In this, the image stride: 14, max image size: 980, and min image size: 378.

Learning. The understanding component of the interleaved formulation outputs the language tokens and is trained using the cross-entropy loss. The text-to-image generation component is trained with the mean-squared error of the rectified flow matching. In our Do-Undo (c) variant we introduce the consistency loss Eq. (1) along with the MSE loss

of flow matching. The weight of consistency loss is set to 0.5 after a grid search in $\{0.4, 0.5, 0.6, 0.8, 1.0\}$.

Hyperparameters. Following BAGEL, we set the maximum number of latent tokens to 64. When training with our data containing a total of 24000 samples, we found the best performance at 14000 steps, given that all the other hyperparameters such as learning rate schedule are same as BAGEL. We train the model on 8 A100 GPUs.

B. Additional Results

Quantitative results. In Sec. and Tab. 6, we present the extended results of Tabs. 1 and 4 from the main paper. In Sec. , we include the zero-shot performance of different models and additionally include the performance of Gemini 2.5. Clearly, Gemini 2.5 is the best performing model for image similarity metrics including DINO-R, DINO-F and EPE based on optical flow. It also demonstrates higher semantic similarity to the prompts as shown in CLIP-T-R and CLIP-T-F. This is further supported by the MLLM as a judge, scores of the samples in Fig. 11, where the per sample scores for Gemini are higher compared to BAGEL. Moreover, when using MLLM as a judge, the Do-Undo approach shows higher per-sample scores compared to Gemini for the reverse images, showing the benefits of our dataset in generating physically aware images. In Tab. 6, we show the performance of different models across 5 seeds when using MLLM as a judge. Here too, we find Gemini to be the best performing model on zero-shot evaluation. FluxKontext a purely image generation model struggles to perform well on physics-aware editing.

In Fig. 12, we evaluate our approach per sample on the proposed metrics. In row 1, we see that the forward action has been performed, therefore, the DINO-F is high and since the reverse action has not been performed, the DINO-R score is low. The optical flow error (OF-F) which measures the flow error between the ground-truth forward action image and the generated image, is higher in row 1 & 3 compared to row 2, even though the action has been performed in rows 1 & 3. This can be attributed to the variations in the objects and the camera movements. Thus, a single metric does not provide a holistic evaluation for generative image editing. Different metrics tend to penalize different aspects of the generated images. We, therefore, include a human evaluation to support our findings and results Sec. C.

Qualitative results. In Figs. 13 and 14, we provide additional qualitative results of our Do-Undo approach against BAGEL. On out-of-distribution action prompts, in Fig. 13, our approach performs considerably better compared to BAGEL, generating images with “stacked tomato cans” and unstacking them, and also disassembling the mxer (row 3). The Do-Undo dataset thus equips BAGEL with the capability to generate physically plausible images based on actions.

Table 5. **Additional quantitative results.** Comparison of models across metrics proposed in Sec. 4.

Model	type	DINO-R \uparrow	DINO-F \uparrow	CLIP-T-R \uparrow	CLIP-T-F \uparrow	EPE \downarrow	OF-F \downarrow
Gemini	Und&Gen	0.890	0.818	0.315	0.310	0.049	83.3
Qwen (20B)	Und&Gen	0.815	0.770	0.312	0.314	0.114	76.2
Flux Kontext (7B)	Gen	0.776	0.750	0.303	0.299	0.129	69.7
Bagel-think (7B) *	Und&Gen	0.837 ± 0.110	0.813 ± 0.103	0.298 ± 0.039	0.301 ± 0.044	0.128 ± 0.070	85.0 ± 48.5
Do-Undo *	Und&Gen	0.819 ± 0.072	0.807 ± 0.102	0.282 ± 0.043	0.281 ± 0.039	0.134 ± 0.080	89.2 ± 45.8
Do-Undo(c) *	Und&Gen	0.812 ± 0.090	0.807 ± 0.090	0.279 ± 0.042	0.282 ± 0.041	0.133 ± 0.080	86.8 ± 45.3

* Mean and std. deviation across 3 seeds.

Table 6. **Additional evaluation with MLLM as a judge.** Quantitative comparison of different methods on the MLLM as a judge metrics over 5 seeds.

Model	IF-F \uparrow	IF-R \uparrow	IDP-F \uparrow	IDP-R \uparrow	OC-F \uparrow	OC-R \uparrow
Gemini	8.34 ± 1.63	8.01 ± 2.11	9.30 ± 1.14	8.30 ± 1.9	9.43 ± 1.14	8.39 ± 2.07
Qwen (20B)	8.41 ± 1.81	8.00 ± 1.91	8.81 ± 1.49	7.64 ± 1.76	8.93 ± 1.48	7.82 ± 1.89
Bagel-think (7B)	7.83 ± 2.14	7.62 ± 2.21	8.78 ± 1.38	7.57 ± 1.94	8.99 ± 1.30	7.79 ± 2.11
FluxKontext (7B)	7.49 ± 2.10	7.04 ± 2.54	7.51 ± 1.87	6.61 ± 2.42	7.73 ± 2.02	6.74 ± 2.63
Do-Undo	7.81 ± 2.15	7.52 ± 2.2	8.53 ± 1.46	7.50 ± 1.90	8.71 ± 1.52	7.61 ± 2.08

Similarly, in Fig. 14, we show that across different examples, our approach outperforms baseline BAGEL in terms of object consistency and action prompt following capabilities.

C. Human Evaluation

Table 7. **Human evaluation.** User study results show that our method is preferred for physics-aware action generation over BAGEL.

Method	Preference (%)
Do-Undo	58.3
Do-Undo(c)	33.3
BAGEL	41.6

In addition to introducing different metrics, we also perform a human evaluation to assess the performance of our approach (Do-Undo), with consistency (Do-Undo(c)) and the baseline BAGEL. We present the participants with 48 instances consisting of forward and reverse action images collecting a total of 336 responses. We instruct to score the images based on if the action is performed and on the object consistency. The participants are asked not to penalize the camera movements with respect to the ground-truth input image and the image quality (for blurry images). We find that our method is preferred over BAGEL for action generation and object consistency.











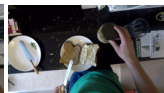






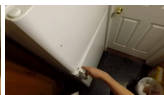






Input Image	Fwd. Image	Gemini		Bagel		Do-Undo(Ours)	
		Forward	Reverse	Forward	Reverse	Forward	Reverse
							
		IF:7	IF:8	IF:10	IF:9	IF:7	IF:10
		IDP:5	IDP:7	IDP:10	IDP:8	IDP:8	IDP:10
		TC:7	TC:8	TC:10	TC:9	TC:7	TC:10
		OC:5	OC:8	OC:10	OC:9	OC:8	OC:10
<p>Forward prompt: From an overhead view, a hand in a blue sleeve uses both hands to securely close a blue and white supplement container with a white lid on a cluttered wooden kitchen counter. Nearby, a green perforated lid, a black cup with white powder, a silver shaker, and a red-handled tool are visible under warm ambient light.</p> <p>Reverse prompt: From a first-person perspective, a person's hands, one with a blue sleeve, remove the white lid from a blue and white supplement container on a cluttered wooden kitchen countertop. The scene includes a purple appliance, a green strainer, and other kitchen items under natural daylight</p>							
							
		IF:10	IF:8	IF:0	IF:0	IF:7	IF:10
		IDP:10	IDP:10	IDP:10	IDP:0	IDP:8	IDP:10
		TC:10	TC:10	TC:0	TC:0	TC:7	TC:10
		OC:10	OC:10	OC:10	OC:0	OC:8	OC:10
<p>Forward prompt: From an overhead view, a person's hand closes the lid on a small glass jar of hummus, positioned on a black countertop next to a plate with two slices of bread and a knife with a yellow handle.</p> <p>Reverse prompt: From an overhead view in a kitchen, a person in a green shirt opens the lid of a small glass jar of hummus on a black countertop. The jar sits beside a white plate with bread and a knife, with a stovetop visible to the left.</p>							
							
		IF:10	IF:9	IF:10	IF:9	IF:7	IF:9
		IDP:10	IDP:8	IDP:8	IDP:7	IDP:9	IDP:8
		TC:10	TC:9	TC:10	TC:8	TC:8	TC:9
		OC:10	OC:8	OC:8	OC:8	OC:9	OC:8
<p>Forward prompt: From an egocentric perspective, a person's right hand closes a white refrigerator door, its interior shelves with bottles and a yellow container now hidden. The left hand holds a small white container with a red label. The scene is set against a white door with a gold handle, on a dark floor, under bright overhead lighting.</p> <p>Reverse prompt: From an egocentric view, a right hand opens the lower white refrigerator door, revealing its illuminated interior with shelves and a freezer compartment. The scene is a dimly lit kitchen with a white door and gold handle to the right, a black floor mat, and a white trash can with a plastic bag nearby.</p>							

Figure 11. **MLLM as a judge.** Qualitative results and the per sample scores from the MLLM as a judge for zero-shot evaluation on Gemini, BAGEL, and our approach. DoUndo (c) generally performs the action accurately almost retaining object identity as seen in (1) & (3) however at times the object consistency is missed.







Input Image (I_o)	Fwd.(Image I_F)	Forward (\hat{I}_F)	Reverse (\hat{I}_R)	OF-F (I_F, \hat{I}_F)	OF-R (I_o, \hat{I}_R)	EPE($I_o, \hat{I}_F, \hat{I}_R$)
						
DINO-F: 0.798 DINO-R: 0.686 CLIP-T-F: 0.257 CLIP-T-R: 0.326 OF-F:86.17 EPE: 0.093						
Forward prompt: From an egocentric view, a right hand pulls open a white refrigerator door, revealing shelves stocked with a loaf of bread, a wooden bowl, and various jars. The scene is a dimly lit kitchen with a dark countertop to the left, holding a white sphere and a box, and a brown tray with an orange fruit below.						
Reverse prompt: From an egocentric view, a right hand pushes the white refrigerator door inward, closing it. The door's white handle is gripped as the interior, filled with bread, a wooden bowl, jars, and a milk carton, is concealed. To the left, a microwave sits on a countertop beside a white sphere and a box. The scene is dimly lit with artificial light.						
						
DINO-F: 0.668 DINO-R:0.748 CLIP-T-F: 0.239 CLIP-T-R: 0.223 OF-F:50.56 EPE: 0.184						
Forward prompt: From a first-person perspective, a light-skinned right hand reaches down to a lower kitchen cabinet under a dark gray countertop. The hand grasps the silver handle and pulls the door open to the left, revealing the dark cabinet interior and the polished wooden floor below. The scene includes a stainless steel oven and a sink with a white container and red utensil, under bright overhead lighting.						
Reverse prompt: From an egocentric view, a light-skinned right hand pushes a silver metal cabinet handle to the right, closing the white cabinet door. The cabinet, above a warm brown wooden floor with a bright light reflection, conceals its dark interior as the door shuts, revealing a kitchen counter and sink in the background.						
						
DINO-F: 0.825 DINO-R:0.648 CLIP-T-F: 0.222 CLIP-T-R: 0.294 OF-F:116.03 EPE: 0.196						
Forward prompt: From an eye-level perspective, a hand firmly pulls open the bottom drawer of a large white cabinet in a cluttered, dimly lit living space. The drawer reveals a chaotic assortment of utensils, including colorful plastic spoons and metal cutlery, amidst the beige carpeted floor scattered with a red and white bag and other items.						
Reverse prompt: From an egocentric view in a cluttered, dimly lit kitchen, a hand firmly pushes a white drawer closed from the bottom, concealing a disorganized mix of colorful plastic spoons (red, yellow, blue), metal spoons, and a white ladle. The drawer is part of a larger white cabinet, with scattered bags and papers on the carpeted floor in the background.						

Figure 12. **Qualitative analysis of similarity metrics.** Qualitative analysis of the optical flow for the forward image (OF-F), optical flow for the reverse image (OF-R) and the end point error (EPE) metric.

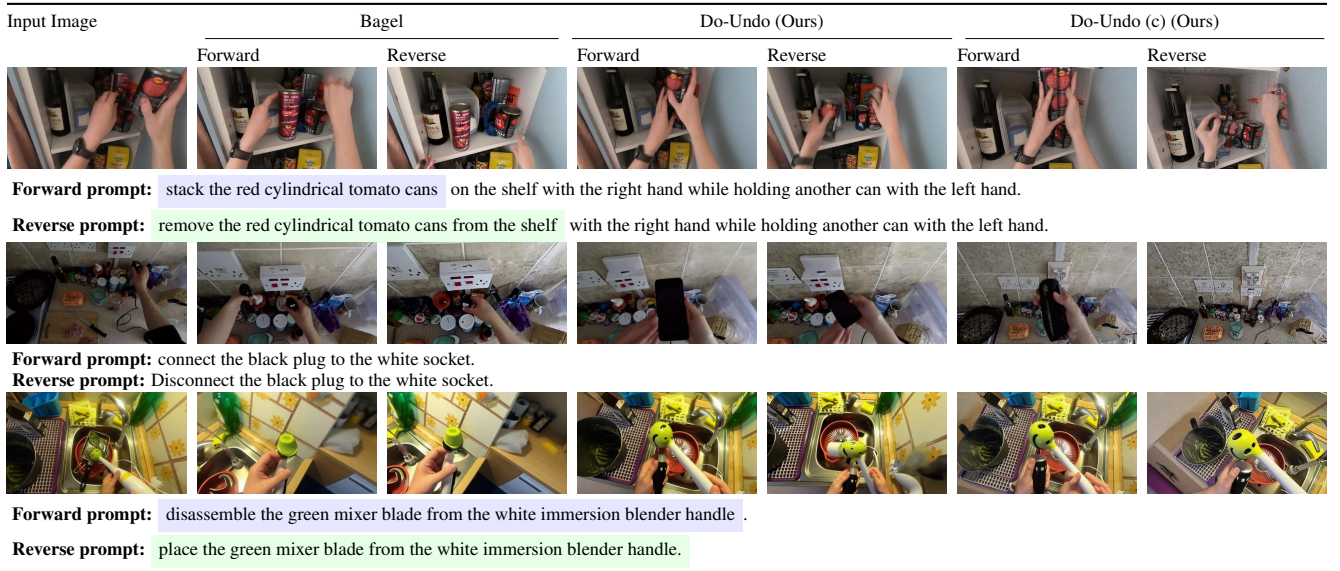


Figure 13. **Qualitative results on out-of-distribution data.** Qualitative comparison BAGEL [10] with Do-Undo (Ours) *i.e.* BAGEL trained with our training data; and Do-Undo(c) with our training data and the consistency loss on out-of-distribution actions.

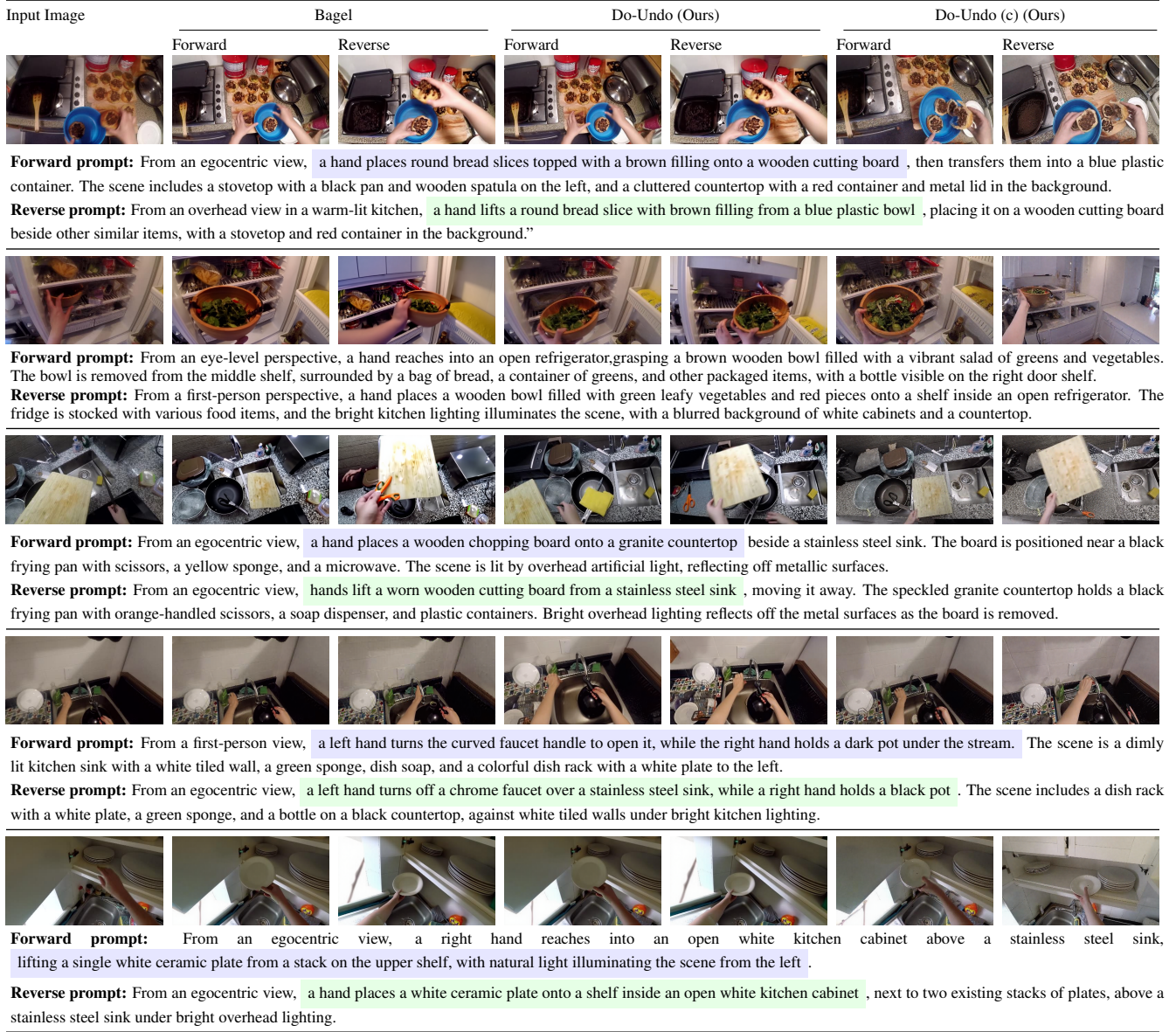


Figure 14. **Qualitative results.** Qualitative comparison BAGEL [10] with Do-Undo (Ours) *i.e.* BAGEL trained with our training data; and Do-Undo(c) with our training data and the consistency loss for physics-aware reversible generation with our prompt expansion. Row (1) DoUndo (c) adds a new slice of bread. Row (2) Do-Undo (c) is the only model that accurately generates "place" action however, details about the refrigerator is lost. Row (3) Gemini also generates a distorted scissors picked up with the board. Row (5) DoUndo (c) performs the undo action placing the plate back